PHYSICAL REVIEW B **81**, 161304(R) (2010)

Probe and control of the reservoir density of states in single-electron devices

M. Möttönen,[1,2,3] K. Y. Tan,[1] K. W. Chan,[1] F. A. Zwanenburg,[1] W. H. Lim,[1] C. C. Escott,[1] J.-M. Pirkkalainen,[1,2] A. Morello,[1] C. Yang,[4] J. A. van Donkelaar,[4] A. D. C. Alves,[4] D. N. Jamieson,[4] L. C. L. Hollenberg,[4] and A. S. Dzurak[1]

[1]*Australian Research Council Centre of Excellence for Quantum Computer Technology, School of Electrical Engineering & Telecommunications, University of New South Wales, Sydney, New South Wales 2052, Australia*

[2]*Department of Applied Physics/COMP, School of Science and Technology, Aalto University, P.O. Box 15100, 00076 Aalto, Finland*

[3]*Low Temperature Laboratory, School of Science and Technology, Aalto University, P.O. Box 15100, 00076 Aalto, Finland*

[4]*Centre for Quantum Computer Technology, School of Physics, University of Melbourne, Melbourne, Victoria 3010, Australia*

(Received 6 October 2009; revised manuscript received 15 December 2009; published 8 April 2010)

We present a systematic study of the density of states (DOS) in electron accumulation layers near a Si-SiO_2 interface. In the experiments we have employed two conceptually different objects to probe DOS, namely, a phosphorus donor and a quantum dot, both operating in the single-electron tunneling regime. We demonstrate how the peaks in reservoir DOS can be moved in the transport window independently of the other device properties. This method introduces a fast and convenient way of identifying excited states in these emerging nanostructures.

DOI: 10.1103/PhysRevB.81.161304 PACS number(s): 73.21.−b, 61.72.uj

The appearance of discrete energy spectra is often regarded as a fundamental property of quantum systems. However, the limit of vanishing energy spacing can be met in many mesoscopic systems at the interface of the quantum and classical regimes, meaning that the energy levels can be treated as a continuum. This gives rise to the concept of density of states (DOS), the integral of which over an energy domain yields the number of quantum states in that region. The DOS concept has been successfully applied in explaining transport, absorption and emission, and quantum statistical phenomena in such devices.[1] In particular, DOS is a key element in the low-temperature behavior of metal-oxide-semiconductor field-effect transistors (MOSFETs) (Ref. 2) which constitute the cornerstone of information processing circuits today. Since device miniaturization has now reached the point where quantum effects of single atoms can dominate the operation characteristics,[3–6] there is an urgent need to understand and distinguish continuum DOS effects from the discrete quantum behavior. In this Rapid Communication, we present a systematic study of the reservoir DOS in two gated MOSFET nanostructures with quantum channels defined by either a quantum dot or the extreme case of a single donor atom.

In a silicon MOSFET a positive gate voltage is applied to induce an electron layer directly below the Si-SiO_2 interface. Hence, the electron dynamics is essentially limited to two dimensions, leading ideally to a constant DOS. In a narrow channel, however, the continuum approximation is only valid in the longest direction, giving rise to quasi-one-dimensional (Q1D) DOS with highly nonuniform characteristics, see Fig. 1(a). Conductance modulations attributed to Q1D density of states were first observed in a parallel configuration of 250 narrow MOSFET channels[7] and later in a single channel.[8–10] Since the cumulative conductance through all occupied states was measured in these experiments, the studies were limited to rather low electron densities in the channel. The density of states is also intimately related to ballistic electron transport through quantum point contacts[11–13] and has been probed in single carbon nanotubes using scanning tunneling microscopy.[14,15]

In single-electron transport through discrete quantum states,[1] the current is directly proportional to the reservoir DOS at a given energy, see Fig. 1. Considerable effort has been directed toward the study of local density of states of a reservoir in the vicinity of an impurity atom in a GaAs quantum well.[16–18] Here, the local DOS was dominated by disorder due to impurity scattering, resulting in reproducible but irregular features in the conductance which behaved in a complicated way as a function of magnetic field. Thus the term local DOS fluctuation was introduced. In our case, the behavior is less complicated, and hence we do not refer to peaks in DOS as fluctuations.

In gated devices, local DOS effects have also been observed in tunneling through a vertical quantum dot,[19] for which a schematic stability diagram is shown in Fig. 1(b). Recently, gated quantum dots have attracted great interest due to their tunability, and lines in the stability diagrams not attributed to excited states have been observed in various structures.[20–24] In Refs. 22 and 23, however, these lines were due to phonon modes and in Ref. 24 due to a background charge, whereas in Refs. 20 and 21 they were stated to arise from reservoir DOS but were not studied in detail.

Motivated by the Kane proposal[25] for a quantum computer based on shallow donors in silicon,[26] there has been considerable development in electron transport through gated

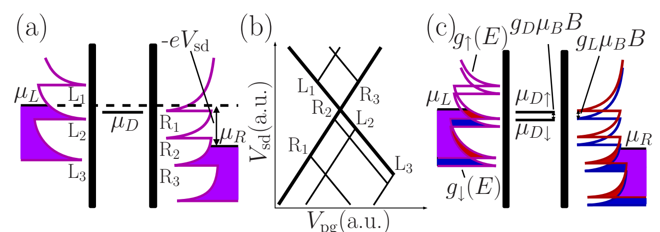

FIG. 1. (Color online) (a) Schematics of single-electron tunneling through a discrete quantum level, μ_D, together with the reservoir Fermi levels, $\mu_{L/R}$, and density of states. (b) Schematic stability diagram showing conductance through the discrete quantum level as a function of the source-drain bias and the plunger gate voltage. The numbered lines of increased conductance arise from the corresponding DOS peaks in panel (a). (c) Zeeman splitting of the reservoir and discrete energy levels in a magnetic field.

 ©2010 The American Physical Society

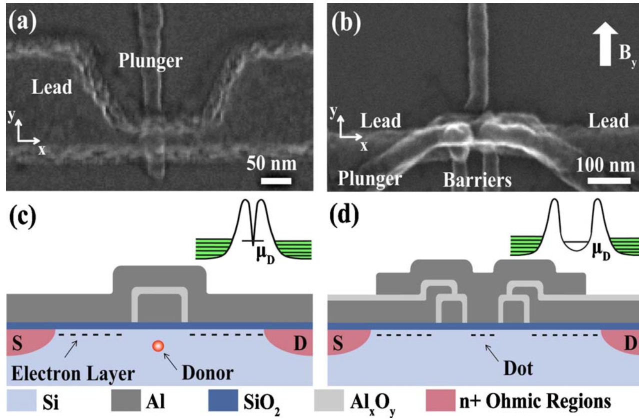

FIG. 2. (Color online) (a) Top view of structure A and (b) structure B and a schematic cross section of (c) structure A and (d) structure B in the $y=0$ plane. The insets show schematic potential landscapes along x.

single donors.[3–6] In these experiments, conductance lines attributed to reservoir DOS have been observed but, again, not studied in detail. Indeed, it has not yet been proven that these features are due to the reservoir DOS. In this Rapid Communication, we present a systematic study of the reservoir DOS in two different nanostructures, namely, in a recently introduced double-gated single-donor transistor[6] (structure A) and in an emerging multigated silicon quantum dot[27] (structure B), shown in Fig. 2. In contrast to previous studies, the double-gated and multigated designs allow us to map conveniently the reservoir DOS at a wide range of energies and electron densities.

The high-purity [001] silicon substrates for both device structures went through similar fabrication steps to those described in detail in Ref. 6. In structure B, however, there are three layers of metallic gates deposited with no implanted donors underneath. The working principle of both devices is that an accumulation layer of electrons is induced directly below the Si-SiO_2 interface using the lead gate voltage V_{lg}. This layer constitutes the reservoirs for single-electron tunneling through a single donor or a quantum dot, the electrochemical potentials of which can be tuned by the plunger gate voltage V_{pg}. For structure A, the plunger gate works also as a barrier gate, depleting the reservoirs in the vicinity of the donor. For structure B, however, we have separate barrier gates which can be used to tune the coupling of the quantum dot to the left and right reservoir independently. The electron densities in the reservoirs can also be controlled independently, but for simplicity, we keep them at the same value here. As the plunger gate voltage is increased, the electrochemical potential of the donor or dot, μ_D, shifts down, eventually entering the source-drain bias window leading to single-electron tunneling through the device, see Figs. 1(a) and 1(b).

The sequential tunneling rate is directly proportional to the reservoir density of states, which leads to a peak in the source-drain current if μ_D is aligned with a peak in the density of states. Critically in our devices, we can shift the Fermi levels of the reservoirs with respect to the conduction band minima by changing the lead gate voltage, V_{lg}, which in turn moves the DOS peaks with respect to the transport window.

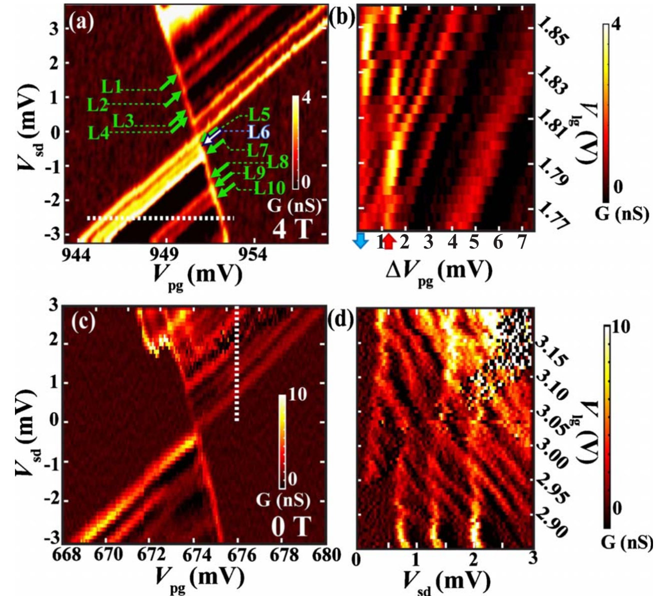

FIG. 3. (Color online) Conductance of (a) structure A with $V_{lg}=1.87$ V and $B=4$ T and (c) structure B with $V_{lg}=3.00$ V, $V_{lb}=0.52$ V, $V_{rb}=0.68$ V, and $B=0$ T as a function of the source-drain bias and the plunger gate voltage. The dashed line in panel (a) represents the trace shown in panel (b) for $V_{sd}=-2.5$ mV as a function of the lead gate voltage for differential conductance. Panel (d) corresponds to the dashed trace shown in panel (c) for $\Delta V_{pg}=2.1$ mV from the transport window at $V_{sd}=0$. The capacitive coupling of the lead gate to the donor or the dot has been compensated by the plunger gate, in structure A by finding the Coulomb peak at $V_{sd}=0$ for each trace and in structure B by a voltage shift $-\Delta V_{lg}/80$ at the plunger. The resulting average voltage shift for structure A was $-0.04\times\Delta V_{lg}$.

The effect of the lead gate voltage on μ_D can be compensated by the plunger gate.[28] Therefore, if we observe conductance peaks to shift consistently with V_{lg} in the stability diagram, we can identify them to arise from peaks in the reservoir DOS, clearly distinct from features due to excited states in the dot or donor which do not move with V_{lg}. Previously, DOS peaks have been probed by changing the temperature[18] or magnetic field,[29] both of which also have an impact on the donor or the dot and which are many orders of magnitude slower than the method presented here. In Ref. 21, gate control of DOS is mentioned but no results are presented.

The measurements were carried out in ^{3}He-^{4}He dilution refrigerators below 100 mK temperatures. The conductance was measured using standard lock-in techniques and the direct current was measured from the same signal after low-pass filtering the modulation arising from the 10–50 μV lock-in excitation. For structure B, only the direct current was recorded and the differential conductance was extracted numerically.

Figure 3 shows measured stability diagrams for structures A [panel (a)] and B [panel (d)]. In structure A, the coupling of the donor to the left reservoir is much weaker than to the right reservoir, and hence only lines with positive slopes corresponding to the left reservoir are visible. This is justified by the sequential tunneling model, in which the current

through the device in the 0-1 electron transition is given by $I=2e\Gamma_{\mathrm{in}}\Gamma_{\mathrm{out}}/(2\Gamma_{\mathrm{in}}+\Gamma_{\mathrm{out}})$, where $\Gamma_{\mathrm{in/out}}$ is the in- or out-tunneling rate. Thus the current is determined by the small rate, independent of whether it corresponds to in or out tunneling.

The stability diagrams shown in Figs. 3(a) and 3(c) do not provide enough information to distinguish whether a specific conductance feature is due to the reservoir DOS or an internal excited state. However, the lead-gate-compensated traces shown in Figs. 3(b) and 3(d) reveal the origin of the conductance peaks. Most of the peaks move uniformly with the lead gate voltage and hence correspond to the reservoir DOS. The fact that there are many unequally spaced peaks which all have the same response to the top gate rule out the possibility that they arise from a coupling to a background harmonic oscillator[22,23] or charges.[24] However, Figs. 3(b) and 3(d) shows features that do not move with V_{lg}, appearing as vertical lines. The line 0.4 meV above the ground state in Fig. 3(b) is the excited spin state of the neutral donor orbital ground state in a magnetic field $B=4$ T. The field is applied in-plane with the induced electron layer throughout this work, see Fig. 1(b). Similarly, the vertical lines in Fig. 3(d) are attributed to excited states of the dot.

We concentrate on structure A below since a more detailed study of structure B is given elsewhere.[27] Furthermore, our emphasis is on the features due to the reservoirs. An in-depth study of the device properties and capacitance modeling of structure A is given in Ref. 6.

We have modeled the single-donor device using technology computer-aided design (TCAD) (Ref. 30) taking into account the full three-dimensional geometry of the system. The TCAD model yields $E_F-E_c=(27.3\times\sqrt{V_{\mathrm{lg}}/[\mathrm{V}]}-8.6)$ meV, where E_F is the Fermi level and E_c is the conduction band minimum in the leads. By matching $\Delta(E_F-E_c)/\Delta V_{\mathrm{lg}}$ from this equation with the observation $\Delta(E_F-E_c)/\Delta V_{\mathrm{lg}}=(11.3\pm1.5)$ meV/V [from Figs. 3(a) and 3(b)], we obtain $E_F-E_c=(25\pm5)$ meV and $V_{\mathrm{lg}}=(1.5\pm0.4)$ V in agreement with the expected values.

Let us briefly discuss whether the observed reservoir DOS is Q1D. The Q1D DOS arises in a system which is infinite only in one direction, here chosen as the x direction. For a noninteracting electron gas, the Q1D DOS is given by the sum of the 1D subbands $D_{1\mathrm{d}}(E-E_{y,z})=\sqrt{2m_x}/(\pi\hbar\sqrt{E-E_{y,z}})$, $(E>E_{y,z})$, over the discrete energy spectrum $\{E_{y,z}\}$ in the y and z directions. Here, the peak spacing in the source-drain current (see Fig. 1) corresponds to the energy spacing in $\{E_{y,z}\}$ in the given energy window. The observed peak spacing in Fig. 3(a) is (0.33 ± 0.03) meV around $E_F-E_c=(25\pm5)$ meV obtained from the TCAD model. An agreement with these values can be obtained in the noninteracting electron gas approximation by taking the single-particle potential to be a triangular well $V_z(z)=eF|z|/\Theta(-z)$ in the z direction (Θ is the Heaviside step function), an infinite $W=70$ nm box potential in the y direction, and a semi-infinite box potential in the x direction. Here, we used the electric field in the vicinity of the Si-SiO_2 interface due to the lead gate, F, as a fitting parameter, and obtained $F=3$ MV/m after taking into account the splitting of the sixfold valley degeneracy in silicon due to the different effective masses and valley-orbit coupling. However, the value expected for the electric field is $F\sim10$ MV/m. This disagreement is likely to be due to the fact that the model does not include the full details of the trapping potential such as disorder or the electric field induced by the accumulation layer, i.e., interactions between the electrons. Thus a deeper theoretical analysis is required that is out of the scope of this Rapid Communication. Furthermore, we note that the Q1D DOS model used above predicts very asymmetric peaks and negative differential conductance [see Fig. 1(a)]. This asymmetry is not visible in Fig. 3, partly due to peak broadening, but negative differential conductance is clearly observable in Fig. 3.

Figure 1(c) shows a schematic diagram of how the DOS peaks behave in magnetic field $\mathbf{B}=B\hat{\mathbf{y}}$. The Zeeman effect shifts the kinetic energy at the Fermi level (E_F-E_c) for the spin-down electrons up by $g_L\mu_BB/2$, and vice versa for spin-up electrons. Here, g_L is the electron g factor in the reservoirs and $\mu_B=e\hbar/(2m_0)$. Thus the effect of this term is to shift and split the DOS peaks. However, if the electron g factor for the donor or dot, g_D, is almost the same as g_L, this compensates for the splitting and results only in a downwards shift of the DOS peaks by $g_L\mu_BB/2$ with respect to the transport window. Thus the shift of the DOS peaks for $g_D=g_L$ is expected to be half of what is observed for the Zeeman splitting of the spin degenerate orbital states. In our case, the DOS peaks simply shift and do not split in magnetic field, as demonstrated in Fig. 4, which implies $g_D\approx g_L\approx2$ consistent with previous measurements.[31] In contrast, Zeeman splitting of DOS peaks has been observed in tunneling through a Si shallow donor in a GaAs/AlAs/GaAs junction.[29]

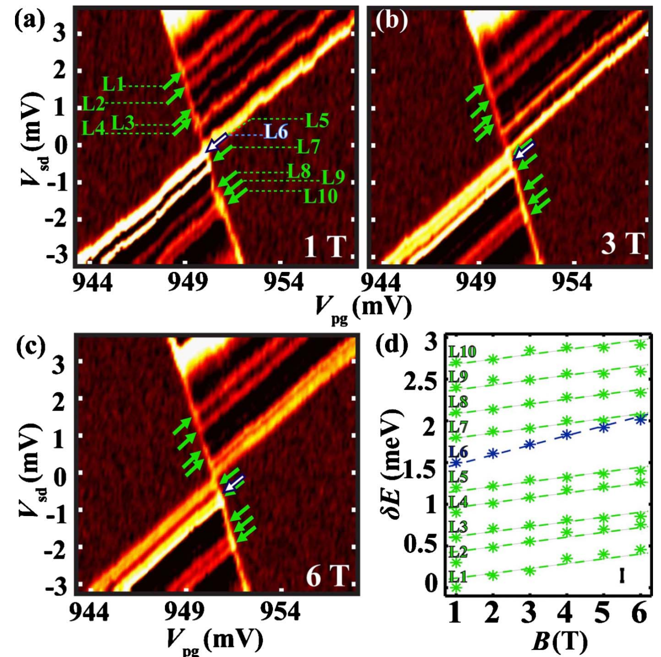

FIG. 4. (Color online) [(a)–(c)] Stability diagrams of structure A in magnetic fields ranging from 1 to 6 T. The spin excited state [L6 in panel (a)] is marked with a white and blue arrow, and the DOS lines are labeled with green arrows. (d) Shift of the conductance lines in magnetic field. Data for each line is offset in energy for clarity. The dashed lines show a slope $2\mu_B$ for L6 and μ_B for the other data.

Figure 4(d) shows the energy shift δE of the conductance peaks with respect to the transport window as a function of magnetic field. We observe that within the estimated error, the shift of the DOS peaks and the spin excited state is in agreement with $\delta E = \mu_B B$ and $\delta E = 2\mu_B B$, respectively. Thus our observations can be explained by the Zeeman effect alone, and they support the interpretation that the conductance peaks which move with the lead gate voltage in Fig. 3 are due to the reservoir DOS.

In conclusion, we have reported detailed studies of the reservoir DOS in nanostructures through gate control of the reservoir electron density. The theoretical models employed are in agreement with the interpretation that the observed conductance features arise from the reservoir DOS but the exact origin of the DOS peaks remains to be proven. Magnetic field spectroscopy of the DOS peaks revealed behavior consistent with energy shifts due to the Zeeman effect alone. Both the single-donor and the quantum dot devices studied exhibited similar conductance patterns arising from the reservoir DOS. Our findings not only confirm the interpretation that additional conductance lines observed previously in transport through single donors[6] are due to reservoir states[3,5] but also demonstrate that these states can be controlled and studied in a quantitative manner.

Note added. We would like to note that in Ref. 27 the observations of the dependence of the shift of the DOS lines as a function of the lead gate voltage and magnetic field are also reported.

The authors thank F. Hudson, D. Barber, and R. P. Starrett for technical support, E. Gauja, A. Cimmino, and R. Szymanska for assistance in nanofabrication, and M. A. Eriksson, J. P. Pekola, and V. Pietilä for insightful discussions. M.M. and J.-M.P. acknowledge Academy of Finland, Emil Aaltonen Foundation, and Finnish Cultural Foundation for financial support. This work was supported by the Australian Research Council, the Australian Government, the U.S. National Security Agency (NSA), and the U.S. Army Research Office (USARO) (under Contract No. W911NF-08-1-0527).

[1] D. V. Averin and K. K. Likharev, in *Mesoscopic Phenomena in Solids*, edited by B. L. Altshuler, P. A. Lee, and R. A. Webb (Elsevier, Amsterdam, 1991), p. 173.

[2] T. Ando, A. B. Fowler, and F. Stern, Rev. Mod. Phys. **54**, 437 (1982).

[3] H. Sellier, G. P. Lansbergen, J. Caro, S. Rogge, N. Collaert, I. Ferain, M. Jurczak, and S. Biesemans, Phys. Rev. Lett. **97**, 206805 (2006).

[4] L. E. Calvet, R. G. Wheeler, and M. A. Reed, Phys. Rev. Lett. **98**, 096805 (2007).

[5] G. P. Lansbergen, R. Rahman, C. J. Wellard, I. Woo, J. Caro, N. Collaert, S. Biesemans, G. Klimeck, L. C. L. Hollenberg, and S. Rogge, Nat. Phys. **4**, 656 (2008).

[6] K. Y. Tan, K. W. Chan, M. Möttönen, A. Morello, C. Yang, J. van Donkelaar, A. Alves, J.-M. Pirkkalainen, D. N. Jamieson, R. G. Clark, and A. S. Dzurak, Nano Lett. **10**, 11 (2010).

[7] A. C. Warren, D. A. Antoniadis, and H. I. Smith, Phys. Rev. Lett. **56**, 1858 (1986).

[8] K. Morimoto, Y. Hirai, K. Yuki, and K. Morita, Jpn. J. Appl. Phys. **35**, 853 (1996).

[9] H. Matsuoka, T. Ichiguchi, T. Yoshimura, and E. Takeda, J. Appl. Phys. **76**, 5561 (1994).

[10] K. Takeuchi and R. Newbury, Phys. Rev. B **43**, 7324 (1991).

[11] B. J. van Wees, H. van Houten, C. W. J. Beenakker, J. G. Williamson, L. P. Kouwenhoven, D. van der Marel, and C. T. Foxon, Phys. Rev. Lett. **60**, 848 (1988).

[12] D. A. Wharam, T. J. Thornton, R. Newbury, M. Pepper, H. Ahmed, J. E. F. Frost, D. G. Hasko, D. C. Peacock, D. A. Ritchie, and G. A. C. Jones, J. Phys. C **21**, L209 (1988).

[13] C. Altimiras, H. le Sueur, U. Gennser, A. Cavanna, D. Mailly, and F. Pierre, Nat. Phys. **6**, 34 (2010).

[14] J. W. G. Wildöer, L. C. Venema, A. G. Rinzler, R. E. Smalley, and C. Dekker, Nature (London) **391**, 59 (1998).

[15] L. C. Venema, J. W. Janssen, M. R. Buitelaar, J. W. G. Wildöer, S. G. Lemay, L. P. Kouwenhoven, and C. Dekker, Phys. Rev. B **62**, 5238 (2000).

[16] J. P. Holder, A. K. Savchenko, V. I. Fal'ko, B. Jouault, G. Faini, F. Laruelle, and E. Bedel, Phys. Rev. Lett. **84**, 1563 (2000).

[17] T. Schmidt, R. J. Haug, V. I. Fal'ko, K. v. Klitzing, A. Förster, and H. Lüth, Phys. Rev. Lett. **78**, 1540 (1997).

[18] T. Schmidt, R. J. Haug, V. I. Fal'ko, K. v. Klitzing, A. Förster, and H. Lüth, Europhys. Lett. **36**, 61 (1996).

[19] L. P. Kouwenhoven, T. H. Oosterkamp, M. W. S. Danoesastro, M. Eto, D. G. Austing, T. Honda, and S. Tarucha, Science **278**, 1788 (1997).

[20] M. T. Björk, C. Thelander, A. E. Hansen, L. E. Jensen, M. W. Larsson, L. R. Wallenberg, and L. Samuelson, Nano Lett. **4**, 1621 (2004).

[21] C. Fasth, A. Fuhrer, L. Samuelson, V. N. Golovach, and D. Loss, Phys. Rev. Lett. **98**, 266801 (2007).

[22] F. A. Zwanenburg, C. E. W. M. van Rijmenam, Y. Fang, C. M. Lieber, and L. P. Kouwenhoven, Nano Lett. **9**, 1071 (2009).

[23] R. Leturcq, C. Stampfer, K. Inderbitzin, L. Durrer, C. Hierold, E. Mariani, M. G. Schultz, F. von Oppen, and K. Ensslin, Nat. Phys. **5**, 327 (2009).

[24] M. Pierre, M. Hofheinz, X. Jehl, M. Sanquer, G. Molas, M. Vinet, and S. Deleonibus, Eur. Phys. J. B **70**, 475 (2009).

[25] B. Kane, Nature (London) **393**, 133 (1998).

[26] R. Vrijen, E. Yablonovitch, K. Wang, H. W. Jiang, A. Balandin, V. Roychowdhury, T. Mor, and D. DiVincenzo, Phys. Rev. A **62**, 012306 (2000).

[27] W. H. Lim, F. A. Zwanenburg, H. Huebl, M. Möttönen, K. W. Chan, A. Morello, and A. S. Dzurak, Appl. Phys. Lett. **95**, 242102 (2009).

[28] An increment in the lead gate voltage also results in a slight increase in the transparency of the tunnel barriers. In structure B, this can be compensated by decreasing the voltage on the barrier gates.

[29] B. Jouault, M. Gryglas, M. Baj, A. Cavanna, U. Gennser, G. Faini, and D. K. Maude, Phys. Rev. B **79**, 041307(R) (2009).

[30] Technology Computer Aided Design modeling package, Integrated Systems Engineering AG, Zurich.

[31] L. H. Willems van Beveren, H. Huebl, D. R. McCamey, T. Duty, A. J. Ferguson, R. G. Clark, and M. S. Brandt, Appl. Phys. Lett. **93**, 072102 (2008).